

Tribological Behavior of Bronze Composite Coatings Obtained by Plasma Thermal Spraying

J. M. Miguel · S. Vizcaino · C. Lorenzana ·
N. Cinca · J. M. Guilemany

Received: 14 May 2010 / Accepted: 23 February 2011 / Published online: 19 March 2011
© Springer Science+Business Media, LLC 2011

Abstract Bronze aluminum composite coatings containing different amounts of alumina were fabricated by plasma spray process and their tribological properties were investigated using ball-on-disk (BOD) and rubber wheel (RW) tests at room temperature. Main wear mechanisms in pure bronze coatings during the ball-on-disk friction test were abrasion and intersplat delamination. The addition of alumina in bronze coatings clearly enhances their wear resistance. To explain this behavior, this article proposes an additional wear mechanism in the composite coatings that involves the rupture of the alumina lamellae located just below the wear track leading to a uniform distribution of fine alumina particles enveloped by the bronze matrix, which increase the surface hardness and hinder the wear. The deposition of debris on the wear track of composite coatings provokes an enhancement of the wear resistance as well. Bronze coatings show a low and stable friction coefficient of around $\mu = 0.3$. Nevertheless, coatings with reinforcing particles of alumina show an abrupt transition in the friction coefficient from values around $\mu = 0.4$ – 0.8 , related to the modification of the surface contacts on the wear track due to the formation of a compacted debris layer deposited during the tribological test.

Keywords Bronze–alumina composites · Structure–properties relationship · Thermal spraying · Wear resistance

1 Introduction

Aluminum–bronze coatings are widely used in navigation, aviation and automotive industries because of their good combination of friction resistance and corrosion properties. These are copper-base alloys containing approximately 5–12% aluminum, some having additions of other elements. High hardness and strength and low friction coefficient are other remarkable characteristics that allow the aluminum bronze to be used in industrial applications as anti-wear coating [1, 2]. Thermal spray is a very successful technique employed to obtain aluminum–bronze coatings, and by means of this technology, the embrittlement caused by the “Self Annealing” phenomenon is avoided [3]. However, in some cases, high abrasion resistance is also required, but its limited hardness makes it very sensible to wear [4]. In order to increase the wear resistance it is possible to use a hard reinforcing phase in the metallic bronze matrix or even, the use of friction modifier fillers for lubricated tribological systems [5]. The reinforcing phase can be in form of continuous fibers or discontinuous particles (e.g., in thermal spraying). Some authors indicate the benefits of the addition of hard particles to modify the tribological properties of bronze coatings. The addition of SiC particles in phosphor-bronze alloys enhances the wear resistance [6]. The addition of TiN and quasicrystal Al-CuFeB particles are used in tin–bronze coatings fabricated by cold spray process to improve their wear resistance [7]. Diamond and WC are also used to increase the tribological properties of Cu-base coatings deposited using thermal spraying technique [8, 9] and the addition of other hard particles produce coatings, which can be used as super-abrasives for grinding minerals and stones [10].

Alumina-metal composite coatings have found increasing industrial use for critical applications because of their

J. M. Miguel (✉) · S. Vizcaino · C. Lorenzana · N. Cinca ·
J. M. Guilemany
Thermal Spray Centre (CPT), University of Barcelona (UB),
Barcelona, Spain
e-mail: chemarimiguel@hotmail.com

unique thermal, mechanical, and electrical properties. Studies in metal–matrix composites of bronze–alumina show that alumina particles improve its strength and wear resistance in both dry and lubricated conditions because of their good interfacial compatibility with the matrix [11]. The effects on the abrasive wear resistance of compositing MMCs of parameters such as volume fraction, Al_2O_3 particle size and porosity have been studied for different abrasive conditions [12, 13]. Thermal sprayed Al_2O_3 –metal coatings give superior mechanical and tribological performances otherwise unobtainable in either constituent material alone [14].

In thermal spraying the particles of powders injected into the flames are submitted to rapid acceleration and intensive heating prior to contact with the substrate. Different spraying methods can be distinguished according to the method of energy generation in the spraying device and the process. Due to the flexibility of the process and the diversity of applicable coating materials, thermal spraying has reached acceptance results in different industries for a wide field of applications, such as wear and/or corrosion applications (glass mold industry, valves, fan blades, etc.), heat insulation, electrical insulation, improvement of electrical conductivity and biocompatible implants [15, 16]. Among the thermal spraying, plasma spraying is very used to obtain ceramic coatings mainly because the high temperature of the plasma (maximum of about 14000 K) allows the powder to melt, obtaining dense coatings, with low porosity and good adhesion with the substrate [17]. The feedstock is injected into the plasma jet, fused and accelerated. During plasma spraying, an arc is ignited between a water-cooled copper anode (nozzle) and a water-cooled tungsten cathode and runs through the plasma gases (Ar, H_2 , He, and/or N_2). The protective effect of the arc plasma, composed by inert gases that limit the direct contact of the sprayed powder with the surrounding atmosphere, allows the production of some metallic coatings with low oxide content. Thus, bronze coatings can be

industrially obtained by plasma spraying [18] as well as by other processes (e.g., High Velocity Oxy-Fuel spraying) for combating the wear and corrosion due to the excellent properties of the obtained coatings [19].

In this study, to enhance the tribological and mechanical properties of pure aluminum bronze deposited using thermal spray, Al_2O_3 is added and the wear properties of the aluminum bronze– Al_2O_3 composite coatings are investigated. In order to compare the results, tribological tests were also carried out on the 34CrMo4 steel substrate, and the values of wear parameters are presented. The impact of the different coatings on the wear resistance is discussed and the tribological mechanisms are described.

2 Experimental Procedure

The powders selected were a commercial aluminum bronze Metco 51NS, manufactured by atomisation and a fused and crushed alumina Metco 101SF. The composition of the aluminum bronze powder is (wt%) 89.70% Cu, 9.24% Al, 0.98% Fe, whereas the alumina is (wt%) 50.83% Al, 0.14% Fe, 0.37% Si, 1.37% Ti, 46.63% O. The particle size distribution, measured using a laser diffractometer (Microtrac model $\times 100/\text{SRA} 150$) was $-125 + 45 \mu\text{m}$ for the aluminum bronze and $-22 + 5 \mu\text{m}$ for the alumina.

Ferritic-perlitic steel 34CrMo4 with a hardness of $\text{HVN}_{100} = 205$ was used as substrate. Substrates were cleaned and grit blasted with Al_2O_3 grade 24 before spraying. The coatings were obtained using a Plasma-Technik A-3000 equipment with an F4 plasma torch in the CPT (Thermal Spray Center, University of Barcelona, Spain). Optimized spray parameters for metallic and composite coatings are listed in Table 1. Three different coatings were obtained with different alumina proportion: Bz (with 0% Al_2O_3), Bz–23% Al_2O_3 , and Bz–38% Al_2O_3 . Two independent injectors were used in order to spray the

Table 1 Spraying parameters

Material	Bronze	Bronze–23%Alumina	Bronze–38%Alumina
Denomination	Bz	Bz–23% Al_2O_3	Bz–38% Al_2O_3
Ar gas(l min^{-1})	54	47	47
H_2 gas(l min^{-1})	9	14	14
Spray distance (mm)	120	120	120
Intensity (A)	500	530	530
Deposited layers	10	10	8
Feeding rate (g min^{-1}) (Bz/ Al_2O_3)	24/0	20/5	20/10
Carrier gas flow (l min^{-1}) (bronze)	3.0	3.0	3.0
Carrier gas flow (l min^{-1}) (alumina)	–	3.4	3.4

Note that both composite coatings are sprayed with the same conditions

bronze and the alumina powders. It is important to note that the standard spraying parameters of bronze were modified to deposit correctly the alumina in the bronze–alumina coatings.

Hardness measurements were carried out at 100 g using a Matsuzawa MXT-OX microhardness tester. Roughness analysis was done in randomly selected areas of the samples. The roughness value R_a (standard deviation with respect to the mean value), R_t (maximum distance between the highest peak and the lowest groove) and R_z (the average peak-to-valley height of the greatest peak-to-valley distances in five consecutive sample lengths) profile were obtained by averaging five sets of data.

Friction tests were carried out using a ball-on-disk (BOD) machine according to ASTM G99-03 procedure (Fig. 1). A martensitic steel ball (AISI 1080) with a hardness $HVN_{100} = 585$ and a WC-6%Co ball with a hardness of $HVN_{100} = 1700$, both of 11 mm in diameter were selected as counterfaces. The environmental conditions were held constant during the test, being the relative humidity and temperature $H_r = 15\text{--}20\%$ and $20\text{ }^\circ\text{C}$, respectively. The sliding distance was kept constant for all the tests at $s = 1000\text{ m}$. A track diameter of $d = 16\text{ mm}$, sliding speed $v = 0.11\text{ m s}^{-1}$, load $F = 15\text{ N}$ and initial coating roughness of $R_a = 0.2\text{--}0.4\text{ }\mu\text{m}$ was used. The wear tracks produced in the coating were studied by SEM (Jeol JSM-5310), the damage produced in the coating was evaluated using Scanning White Light Interferometry (SWLI, Zygo NewView 100) and the results of coating

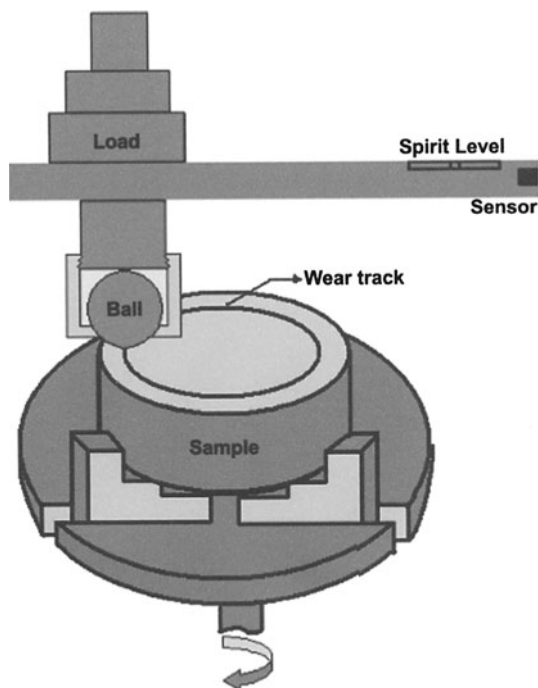


Fig. 1 Ball-on-disk (BOD) equipment according to ASTM G99-03

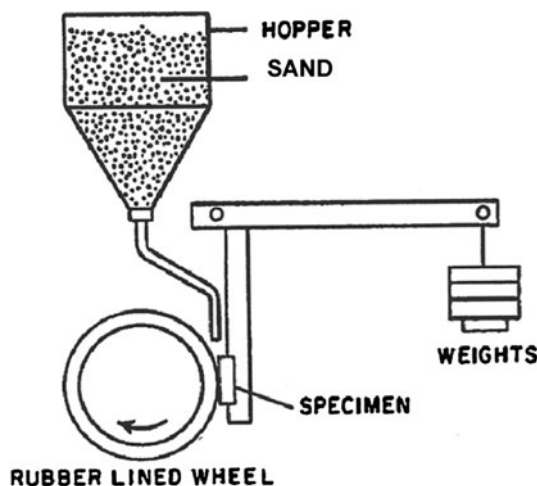


Fig. 2 Rubber wheel (RW) equipment according to ASTM G65-00

volume loss are reported. The porosity and thickness of the coatings were measured by image analysis using software Matrox Inspector.

Abrasion tests were carried out with a rubber wheel test machine using SiO_2 with size comprised between 0.4 and 0.8 mm as abrasive material according to the ASTM G65-00. The rubber wheel rotates at 131 rev min^{-1} (Fig. 2).

Adhesion tests were carried out according the standard test method for adhesion or cohesion strength of thermal spray coatings ASTM C633-01, and the average value of three samples for each reference was reported.

3 Results and Discussion

3.1 Coating Structures

The structures of the coatings are shown in Fig. 3a, b, c. The coatings are composed by a lamellar structure with a low quantity of unmelted particles. Alumina (dark lamellas) is homogeneously distributed in the composite coatings and it is perfectly melted during spraying, indicating that the spraying parameters are correct. In order to melt both powders with the same spraying conditions, an alumina with small particle size was chosen, so it can be completely melted even if it has a relatively high melting point compared to bronze (2350 vs. 1350 K) and lower thermal conductivity ($27\text{ vs. }58\text{ W m}^{-1}\text{ K}^{-1}$) [20].

Main characteristics of the coatings are shown in Table 2. Coatings have a dense structure with a porosity value minor than 1%, which is randomly distributed in the coatings. XRD analysis indicated that the aluminum–bronze is composed by two different phases, AlCu_3 (martensite) and Cu (α -phase), with a high degree of crystallinity (Fig. 4), with good defined peaks and no presence of

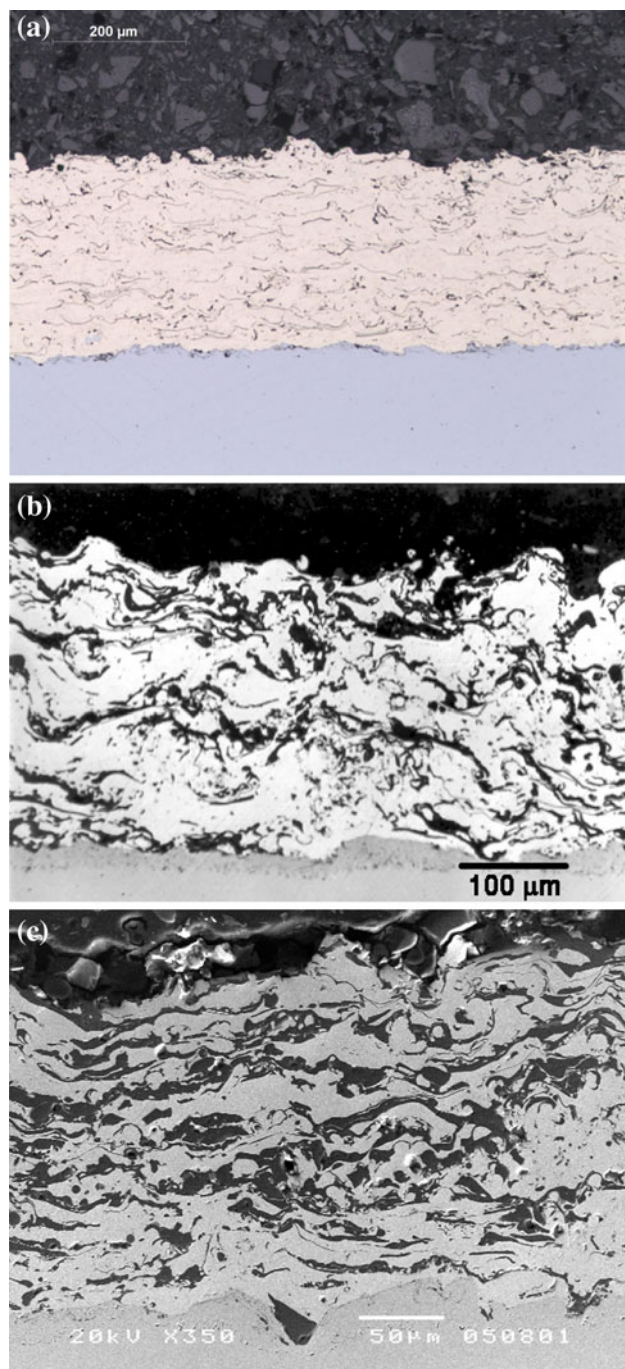


Fig. 3 **a** Structure of the bronze coating, **b** structure of the Bz-23% Al_2O_3 coating. Dark lamellas correspond to Al_2O_3 and **c** structure of the Bz-38% Al_2O_3

amorphous phases. SEM images of the aluminum–bronze lamellas show a fine columnar structure, which corresponds to the β -phase originated at high temperature during thermal spraying, which transform to martensite during the rapid cooling in the coating formation (Fig. 5). Al_2O_3 crystallizes in corundum phase. Cohesion between alumina and bronze particles is good, without either cracks or voids in the

interfaces. We can state that the addition of alumina does not have a detrimental effect on the structure and cohesion of the coating.

The deposited thickness per pass is similar in all the cases (around $25 \mu\text{m pass}^{-1}$). Roughness parameters are even lower with the increase of alumina content in the deposited coatings. Microhardness values enhance with the addition of alumina, so the coating Bz-23 Al_2O_3 has a microhardness value of 209 HVN_{100} (23% higher than the pure bronze) and the coating Bz-38 Al_2O_3 has a microhardness value of 230 HVN_{100} (35% higher than the pure bronze). The adhesion test shows that the addition of alumina improves the adhesion values until a maximum value of 45 MPa for Bz-23 Al_2O_3 . Adhesive rupture (between the coating and the substrate) is shown in all the coatings.

3.2 Abrasion Resistance

Figure 6 displays the weight loss versus time of pure bronze and bronze–alumina composite coatings and the values are compared to the steel substrate tested using ASTM G65-00 (rubber wheel test). To obtain the wear rate ($\text{mm}^3 \text{N}^{-1} \text{m}^{-1}$) plotted in Fig. 7, the used densities are those of bulk materials (7.65, 3.97, and 7.85 g cm^{-3} for bronze, alumina, and steel, respectively).

From these results, it is apparent that the addition of alumina effectively improves the abrasion wear resistance of the pure bronze. Hard alumina particles are useful in decreasing abrasive wear. As the soft bronze matrix is cut away and removed, the load is significantly transferred to the hard alumina particles. Alumina particles wear occurs also by abrasion, but with a lower wear rate.

3.3 Friction Resistance and Wear Mechanisms

Friction resistance was tested with ASTM G99-03 (ball-on-disk) and wear parameters of counterfaces for samples Bz, Bz-23% Al_2O_3 , and Bz-38% Al_2O_3 are indicated in Table 3. Contact diameter of WC-6%Co after the ball-on-disk test is lower than that of the steel counterface. Volume loss of the WC-6%Co does not depend on the tested coating, whereas it has an important role on the wear parameters of the steel counterface. The accepted theory [21, 22] predicts a transition from “hard” to “soft” abrasive behavior when the ratio of hardness of the abrasive to that of the abraded material $H_a/H_m = 1.2$. In the present case, hardness of the abrasive component alumina ($H_a = 1400\text{--}1600 \text{ HVN}$) [20] does not achieve a high enough value to wear the WC-6%Co ($H_m = 1700 \text{ HVN}_{100}$) in “hard” abrasive behavior, and for this reason, even if the alumina content increases, the volume loss of WC-6%Co remains almost unaltered. Nevertheless, it can be considered that the wear of the steel counterface occurs in the

Table 2 Main characteristics of the coatings

	Al ₂ O ₃ (%)	Thickness (μ m)	Number of passes	Thickness (μ m) per pass	Ra/Rt/Rz (μ m)	Porosity (%)	HVN ₁₀₀	Adherence (MPa)
Bz	0	245	10	24.5	17.5/106/87	<1	170 \pm 23	34 \pm 5
Bz-23%Al ₂ O ₃	23	248	10	24.8	16.5/105/83	<1	209 \pm 21	45 \pm 6
Bz-38%Al ₂ O ₃	38	202	8	25.4	13.5/84/70	<1	230 \pm 15	43 \pm 4

Note the differences in the microhardness and adherence values

Fig. 4 XDR image of the bronze coating showing that α -Cu and AlCu₃ are the main phases (without presence of amorphous phase)

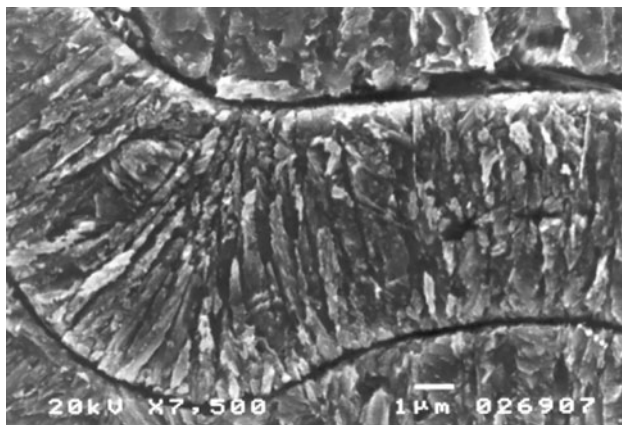
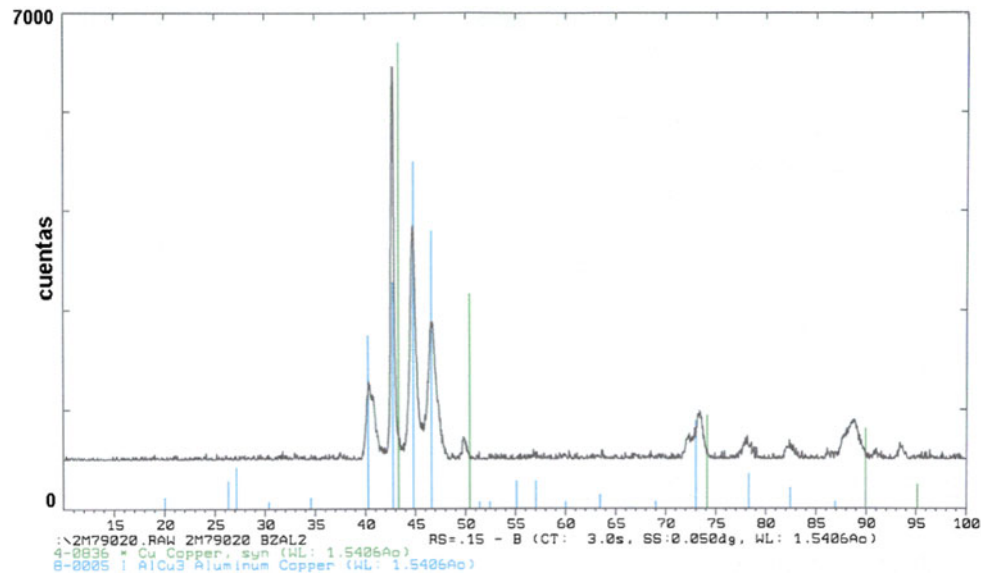


Fig. 5 Chemical etched bronze coating showing the directional grain grown

hard abrasive mode, in which the elimination of the material by the abrasive (alumina) occurs more and more as the alumina content increases. Therefore, it is essential to note the importance in knowing which counterface will be used in real applications, in order to meet the best possible combination and alumina proportion in the composite coating.

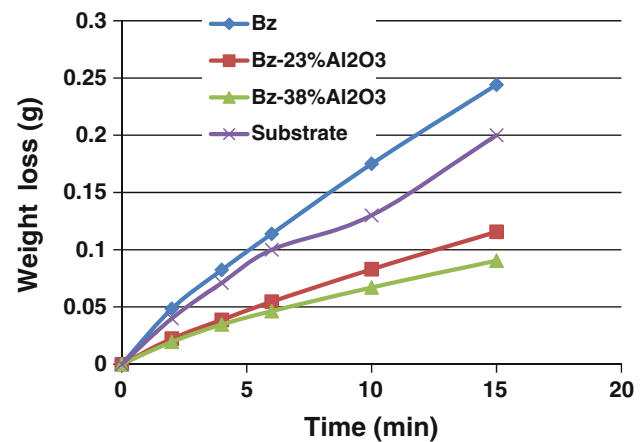


Fig. 6 Weight loss of the coatings and the substrate tested with rubber wheel

Table 4 shows the main wear parameters (volume loss, width and depth of the wear track) of the tested coatings with steel and WC-6%Co counterfaces, analyzed with Scanning White Light Interferometry. As a reference, the values obtained by the steel substrate are also indicated.

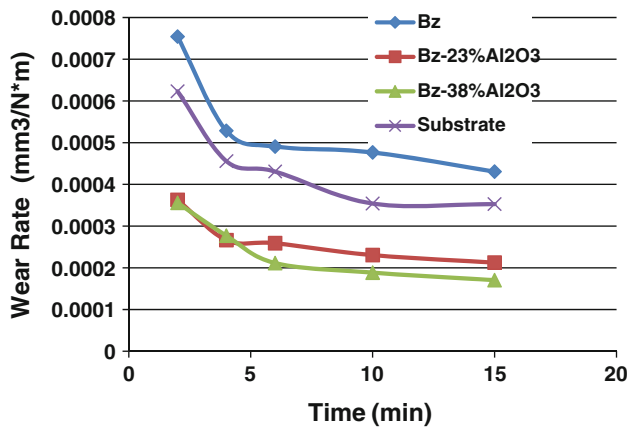


Fig. 7 Wear rate of the coatings tested with rubber wheel. The addition of alumina enhances greatly the wear resistance of the coatings

It is important to remark that increasing the Al₂O₃ content in the tested coatings leads to an important decrease in the volume loss, width, and depth of the wear track. So, the use of 23%Al₂O₃ diminishes in a factor between 2 and 4 (depending of the counterface) the volume loss, whereas the use of 38%Al₂O₃ decreases it in a factor around 5. Thus, it can be concluded that the addition of the hard alumina phase has a beneficial influence on the sliding wear resistance. However, this effect is stabilized with increasing the alumina content, and thus, the presence of 38%Al₂O₃ does not add any further substantial improvement with respect to 23%Al₂O₃ coatings.

SEM analyses were carried out on the wear track of the bronze and the composite coatings at sliding distances of 100 and 1000 m (end of test). Important differences are found in the tribological mechanisms of the pure bronze coatings and the bronze–alumina composite coatings.

During the entire sliding test the bronze surface showed parallel scratches, indicating that abrasion is an important wear mechanism (Figs. 8, 9). This wear mechanism is present when WC-6%Co or steel are used as counterface, because of the lower hardness of the bronze matrix. Cavities with dimensions of around 50–100 μm indicate that surface fatigue (splats delamination) is also an important wear mechanism and it is confirmed by SEM analyses of debris, where big particles are detected (Fig. 10). Splat delamination is one of the most common wear mechanisms in thermal spray processes, also reported by other authors, due to the limited cohesion of the coatings [22]. This mechanism involves intersplat crack propagation until splats are not longer attached and easily removed. Even if spray conditions are acceptable, intersplat cohesion is one of the weakest points of most of the thermal spray coatings [23, 24], caused by the discontinuous solidification process inherent in plasma spraying. Debris produced by this wear mechanism has high dimensions because it comes from the detachment of single splats, though in other cases it could be generated by the elimination of bits of coating containing several splats. The temperature achieved in the friction process (flash temperature) [25] is high enough to produce the oxidation of the surface of the wear track,

Table 3 Wear parameters of the counterfaces

Coating	Counterface	Contact surface diameter (μm)	Volume loss (×10 ⁻⁴ mm ³)	Nominal load (MPa)
Bz	WC-6%Co	1000	89.2	19.1
Bz-23%Al ₂ O ₃	WC-6%Co	1000	89.2	19.1
Bz-38%Al ₂ O ₃	WC-6%Co	1050	108.5	17.3
Bz	Steel	1300	254	11.3
Bz-23%Al ₂ O ₃	Steel	1800	936	5.9
Bz-38%Al ₂ O ₃	Steel	2200	2093	3.9

The increase of alumina content in the composite coatings leads to a bigger wear in the steel counterface

Table 4 Wear parameters (obtained by scanning white light interferometry) of the coatings

Coating	Counterface	Volume loss (mm ³)	Width wear track (mm)	Depth wear track (μm)
Bz	Steel	4.23	1.90	71
Bz-23%Al ₂ O ₃	Steel	1.13	1.28	31
Bz-38%Al ₂ O ₃	Steel	0.80	1.20	27
Steel substrate	Steel	3.1	1.8	50
Bz	WC-6%Co	3.33	1.86	62
Bz-23%Al ₂ O ₃	WC-6%Co	1.60	1.58	33
Bz-38%Al ₂ O ₃	WC-6%Co	0.62	1.22	15
Steel substrate	WC-6%Co	3.05	1.70	55

Volume loss decreases with the addition of alumina

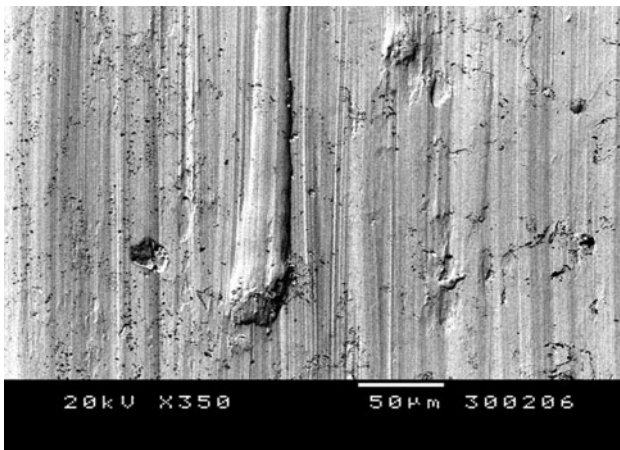


Fig. 8 Wear track of the bronze coating against a steel counterface (sliding distance = 100 m). Abrasion marks are already present

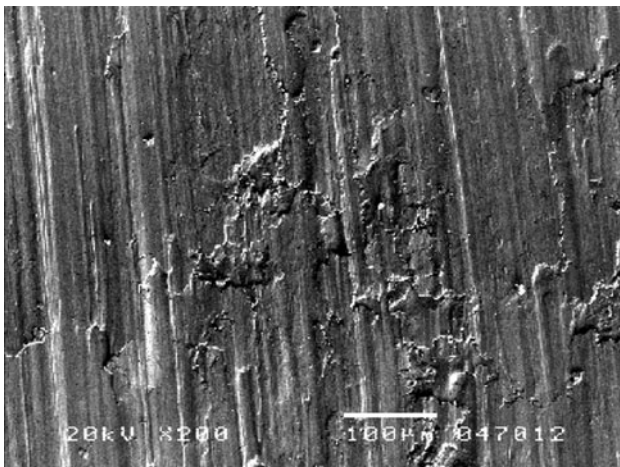


Fig. 9 Wear track of the bronze coating against a steel counterface (sliding distance = 1000 m). Note the high quantity of parallel scratches and cavities (center of the image)

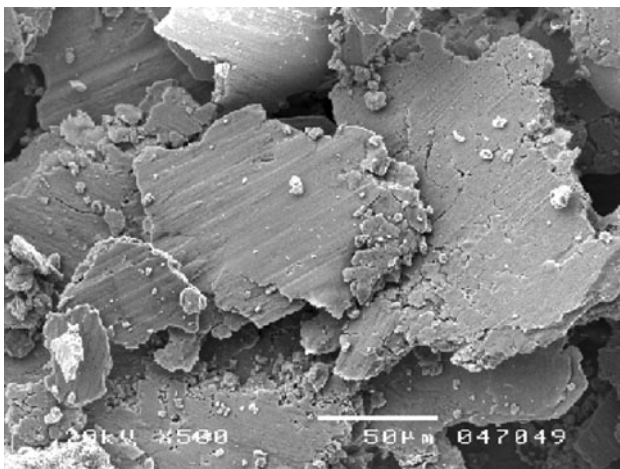


Fig. 10 Debris of the bronze coating is mainly composed by flake-like particles indicating the important role of intersplat delamination

where also deformation and sub-surface cracks are present (Fig. 11).

The wear tracks of the composite coatings show abrasion and intersplat delamination during the entire test. However, the effect of these two processes on the coating damage depends strongly on the sliding distance. Initially (sliding distance = 100 m) these two mechanisms are already present. During sliding, alumina lamellas are broken due to the plastic deformation caused by the applied load on the metal matrix and small alumina particles of size minor than 5 μm are distributed uniformly on the wear track and coating sub-surface (Fig. 12). Cross section of the wear track allows us to observe that these lamellas are not only broken in the surface of the wear track, but also in a depth of 50 μm (Fig. 13). These small alumina particles are good mixed in the bronze matrix and the microhardness value in this area is $\text{HVN}_{100} = 420 \pm 30$, due to the uniform distribution of the small alumina particles combined with the hardening of the deformed bronze. In addition, debris composed of Cu, Al, and O (material detached from the coating and counterface) is deposited on the coating surface, decreasing the damage of the coating surface. Thus, these two above-described processes (Al_2O_3 fracture and mixture with the bronze matrix and debris deposition) decrease the effect of abrasion and intersplat delamination and enhance the wear resistance of the composite coatings. Debris of composite coatings is composed by small particles as well as other big flake-like particles detached due to the fatigue process (Fig. 14). This debris could be the responsible of the difference of depth in the wear track of coatings tested with different counterfaces. Third-body abrasion caused by debris, which is substantially higher when the steel counterface is used, promotes the wear of the coatings.

3.4 Friction Coefficients

Friction coefficients of the bronze–alumina and bronze coatings tested with WC-6%Co and steel balls are plotted in Figs. 15 and 16, whereas the friction parameters, calculated as the average friction value in the last 200 m, are shown in Table 5.

The Bronze coatings show a stable friction coefficient of 0.27 and 0.30, when they are tested with the steel and WC-6%Co counterface, respectively.

The Bz-23% Al_2O_3 coatings show a clear transition from a low friction coefficient of around 0.4 to a high friction coefficient between 0.7 and 0.8, in both tested counterfaces. The Bz-38% Al_2O_3 shows a very similar behavior; however, the transition is produced earlier in the friction test. Thus, this transition from low to high friction coefficient depends on the alumina content and occurs abruptly in a few meters. The wear track was analyzed before and

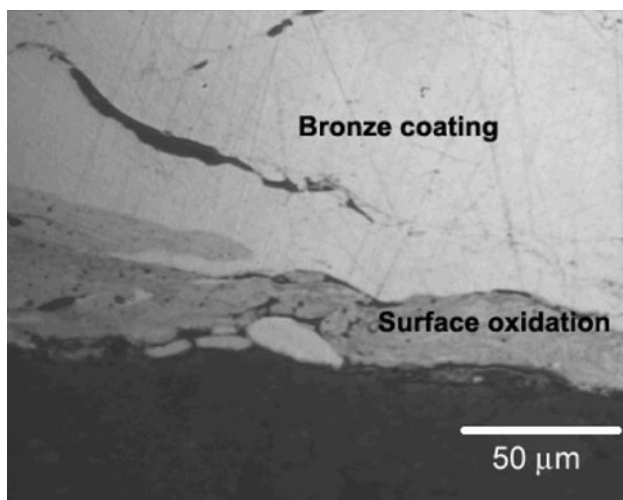


Fig. 11 Cross section of the bronze wear track. Note the oxidation in the surface

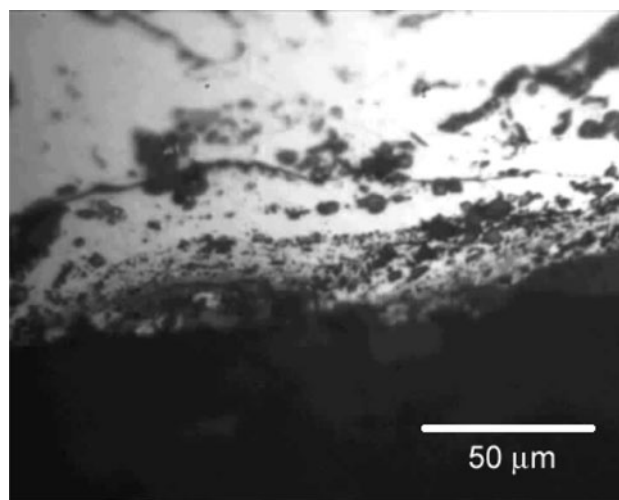


Fig. 13 Cross section of the Bz-23%Al₂O₃ wear track (sliding distance = 1000 m). Note the small dimensions of the broken alumina particles

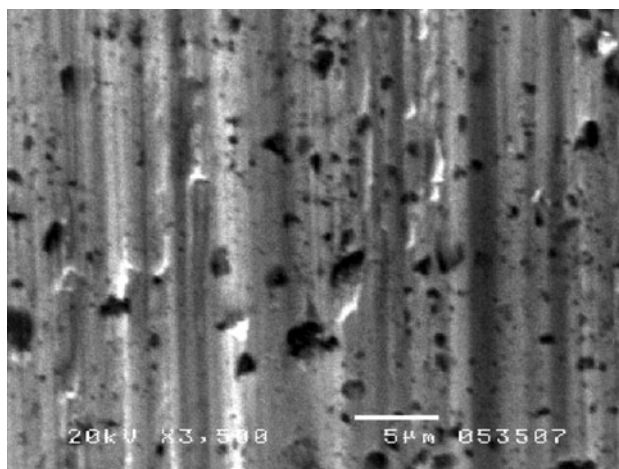


Fig. 12 Wear track of the Bz-23%Al₂O₃ against a steel counterface (sliding distance = 100 m). *Dark particles* of small size Al₂O₃ are distributed homogeneously in the wear track

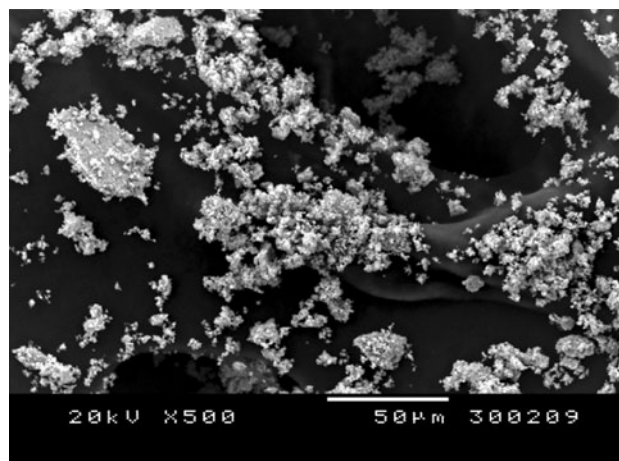


Fig. 14 Debris of Bz-23%Al₂O₃ against a steel ball

after this transition. In the region where low friction coefficient exists, the wear track shows scratches and holes due to the intersplat delamination process, but it is free from debris (Fig. 12). In the region where high friction coefficient exists, there is a rough wear track and a high quantity of deposited debris (Fig. 17). This rough worn surface, composed mainly by aluminum and copper oxides, makes difficult the movement of the counterface, leading to the high friction value.

Figure 18 explains the relationship between friction coefficients and wear mechanisms along the sliding wear test. Abrasion and intersplat delamination are the common tribological mechanisms that occur during the entire test in bronze and composite coatings. When they are present, without deposition of debris, the friction coefficient is low ($\mu = 0.3$ – 0.4). However, the two other suggested processes

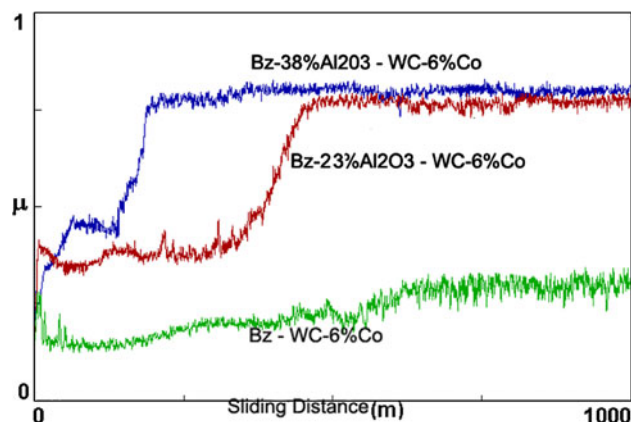


Fig. 15 Friction coefficient of the coatings against a WC-6%Co counterface

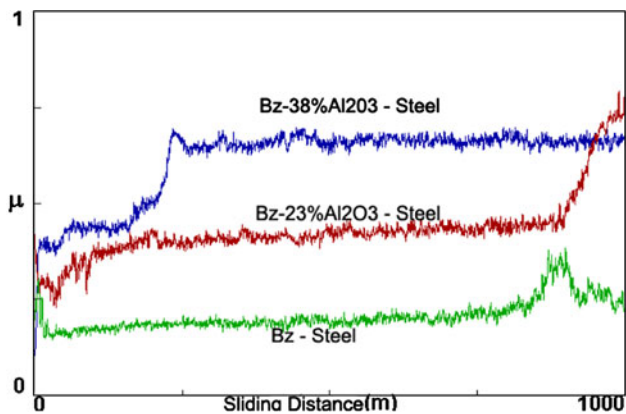


Fig. 16 Friction coefficient of the coatings against a steel counterface

Table 5 Mean friction coefficient (μ) of the coatings (obtained as the average of the 200 m last meters of the ball-on-disk test)

	Bz	Bz-23%Al ₂ O ₃	Bz-38%Al ₂ O ₃
WC-6%Co	0.30	0.77	0.80
Steel	0.27	0.54	0.66

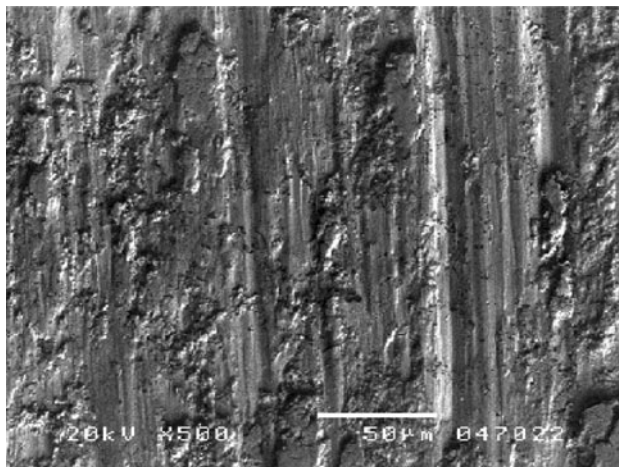


Fig. 17 Wear track of the Bz-23%Al₂O₃ against a steel ball. Note the debris on the coating surface. EDS analysis showed that debris is composed by Cu, Al, and Fe oxides

that occur only in the composite coatings (alumina rupture and debris deposition) prevent the damage of the wear track. Alumina particles are broken, partially detached from the coating surface, and finally, debris composed by alumina and partially oxidized material from the counterface and matrix of the coating is finally deposited on the wear track. When debris deposition is completed, the friction coefficient is high ($\mu = 0.8$).

4 Conclusions

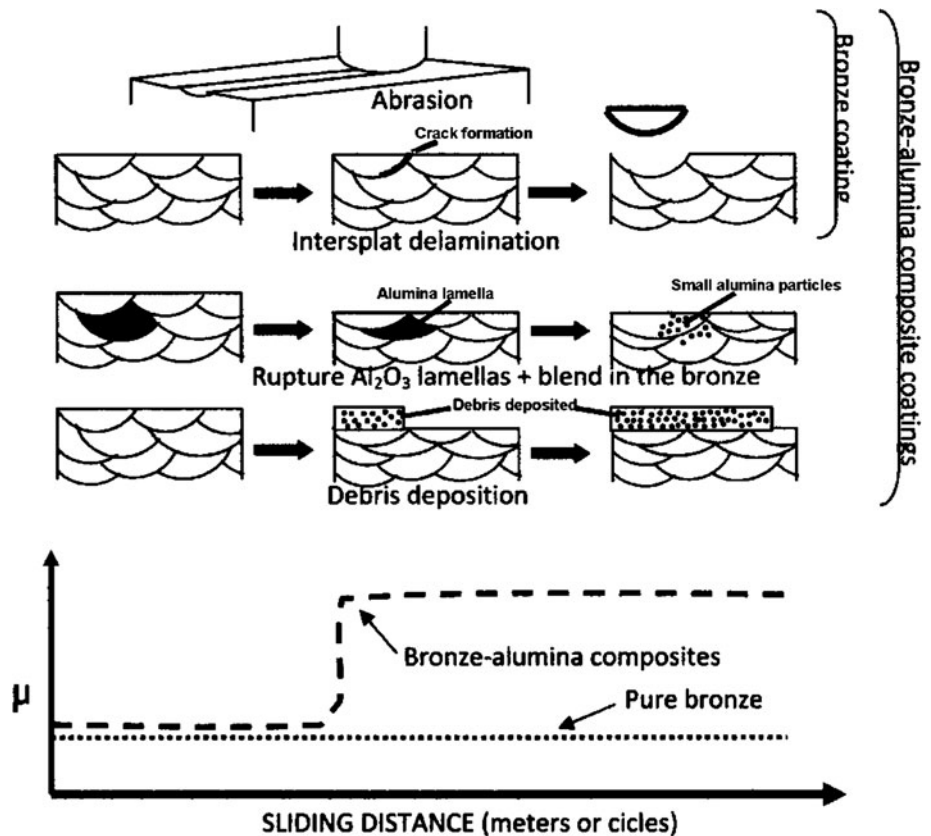
Bronze–alumina composite coatings can be successfully obtained by plasma spraying with significant improved tribological and mechanical properties when compared with pure bronze coatings. The use of optimized spraying parameters (which allows the two sprayed powders to melt) produces dense composite coatings with good adhesion. Experimental investigation showed that the addition of alumina to bronze coatings is responsible for a general increase in abrasion resistance (with a plateau effect of %Al₂O₃) accompanied by an increased of friction coefficient.

Bronze coatings show good friction properties ($\mu = 0.3$) that remains constant during the entire test. The addition of alumina provokes important modifications in the friction coefficient and an abrupt transition from $\mu = 0.4$ to 0.8 is found. The reason of these different friction values corresponds to different surface contacts between the counterface and the composite coatings. Whereas in the first region (low friction coefficient, $\mu = 0.4$) a direct contact between the counterface and the worn coating surface exists, the second region (high friction coefficient, $\mu = 0.8$) corresponds to a contact between the counterface and the deposited debris.

SEM analysis of the debris and the wear track confirmed differences in the main wear mechanisms during ball-on-disk tests of pure bronze coatings and the composite coatings. Whereas pure bronze coatings show abrasion and intersplat delamination as main wear processes (with no deposition of debris on the wear track), the composite coatings show two additional processes that diminish the wear of the coatings: rupture of the alumina lamellas and debris deposition. Thus, during sliding, the alumina lamellas are broken and finely distributed in the soft bronze matrix, promoting the microhardness value in the worn surface (420 HVN₁₀₀). In addition, debris composed of copper and aluminum oxides is deposited on the wear track, decreasing the wear of the coatings. These two wear mechanisms described above are very important because allow the improvement of the tribological properties of soft and ductile materials with the addition of hard and wear resistant lamellar-like phases (Al₂O₃ in this case).

Depending on the application, an optimal composition of the composite coatings must be selected, in order to obtain the optimum of friction coefficient and wear resistance. A further study of other similar combination of spray powders will be done in order to have a better understanding of the possibilities that open these tribological processes.

Fig. 18 Tribological processes during the wear sliding process (BOD test)



Acknowledgments The authors would like to thank the Generalitat de Catalunya -project 2009SGR00390.

References

- Zhong-li, Z., De-yuan, L., Shui-yong, W.: High temperature performance of arc-sprayed aluminum bronze coatings for steel. *Trans. Nonferrous Met. Soc. China* **16**, 868–872 (2006)
- Kudashov, D.V., Zauter, R., Müller, H.R.: Spray-formed high-aluminium bronzes. *Mater. Sci. Eng. A* **477**, 43–49 (2008)
- Alam, S., Saraki, S., Shimura, H.: Friction and wear characteristics of aluminum bronze coatings on steel substrates sprayed by a low pressure plasma technique. *Wear* **248**, 75–81 (2001)
- van der Heide, E., Stam, E.D., Giraud, H., Lovato, G., Akdut, N., Clarysse, F., Caenen, P., Heikillä, I.: Wear of aluminium bronze in sliding contact with lubricated stainless steel sheet material. *Wear* **261**, 68–73 (2006)
- Tura, J.M., Traveria, A., de Castellar, M.D., Pujadas, J., Blouet, J., Gras, R., Magham, H.G., Belair, P., Hanau, T., Romero, A.: Frictional properties and wear of a molybdenum coating and a bronze (Cu–10%Sn) with friction modifier fillers. *Wear* **189**, 70–76 (1995)
- Sharma, S.C., Satish, B.M., Girish, B.M., Somashekar, D.R.: Wear characteristics of phosphor-bronze/silicon carbide particulate composites. *J. Mater. Process. Technol.* **118**, 65–68 (2001)
- Guo, X., Zhang, G., Li, W., Gao, Y., Liao, H., Coddet, C.: Investigation of the microstructure and tribological behavior of cold-sprayed tin-bronze-based composite coatings. *Appl. Surf. Sci.* **255**, 3822–3828 (2009)
- Venkateswarlu, K., Rajinikanth, V., Naveen, T., Prasad, D., Atiqzaman, S., Kumar Ray, A.: Abrasive wear behavior of thermally sprayed diamond reinforced composite coating deposited with both oxy-acetylene and HVOF techniques. *Wear* **266**, 995–1002 (2009)
- Venkateswarlu, K., Ray, A.K., Gunjan, M.K., Mondal, D.P., Pathak, L.C.: Tribological wear behavior of diamond reinforced composite coating. *Mater. Sci. Eng. A* **418**, 357–363 (2006)
- Tillmann, W., Vogli, E., Nebel, J.: Development of detonation flame sprayed Cu-base coatings containing large ceramic particles. *J. Therm. Spray Tech.* **16**(5–6), 751–758 (2007)
- Sornakumar, T., Senthil Kumar, A.: Machinability of bronze-alumina composite with tungsten carbide cutting tool insert. *J. Mater. Process. Technol.* **202**, 402–405 (2008)
- Yilmaz, O., Buytoz, S.: Abrasive wear of Al₂O₃-reinforced aluminium-based MMCs. *Compos. Sci. Technol.* **61**, 2381–2392 (2001)
- Travitzky, N.A.: Microstructure and mechanical properties of alumina/copper composites fabricated by different infiltration techniques. *Mater. Lett.* **36**, 114–117 (1998)
- Hung, J.H.H., Chiu, Y.L., Liang, J.: Reciprocating wear properties of thermal sprayed titanium aluminide-alumina composite coatings. *Surf. Coat. Technol.* **202**, 5599–5602 (2008)
- Miguel, J.M., Guilemany, J.M., Vizcaino, S.: Tribological study of NiCrBSi coating obtained by different processes. *Tribol. Int.* **36**, 181–187 (2003)
- Steinhäuser, S., Wielage, B., Hofmann, U., Schnick, Th., Ilyuschenko, A., Azarova, T.: Plasma-sprayed wear-resistant coatings with respect to ecological aspects. *Surf. Coat. Technol.* **131**, 365–371 (2000)
- Pawlowski, L.: *The Science and Engineering of Thermal Spray Coatings*, pp. 33–35. Wiley, New York (1992). ISBN 0 471 95253 2
- Jose, M.: Miguel, Propiedades mecánicas y tribológicas de recubrimientos de proyección térmica. PhD thesis, Barcelona (Feb 2002)

19. Tan, K.S., Wharton, J.A., Wood, R.J.K.: Solid particle erosion–corrosion behaviour of a novel HVOF nickel aluminium bronze coating for marine applications—correlation between mass loss and electrochemical measurements. *Wear* **258**, 629–640 (2005)
20. ASM International: *Metals Handbook, Properties and Selection: Nonferrous Alloys and Special-Purpose Materials*, vol. 2, 10th edn. ASM International, Materials Park, OH (2006). ISBN 0-87170-378-3
21. ASM International: *Metals Handbook, Friction, Lubrication and Wear Technology*, vol 18, 10th edn. ASM International, Materials Park, OH (2006). ISBN 0-87170-378-3
22. Tabor, D.: The physical meaning of indentation and scratch hardness. *Br. J. Appl. Phys.* **7**, 159–166 (1956)
23. Erickson, L.C., Westergard, R., Wiklund, U., Axén, N., Hawthorne, H.M., Hogmark, S.: Cohesion in plasma-sprayed coatings—a comparison between evaluation methods. *Wear* **214**, 30–37 (1998)
24. Prchlik, L., Sampath, S.: Effect of the microstructure of thermally sprayed coatings on friction and wear response under lubricated and dry sliding conditions. *Wear* **262**, 11–23 (2007)
25. Kalin, M.: Influence of flash temperatures on the tribological behaviour in low-speed sliding: a review. *Mater. Sci. Eng. A* **374**, 390–397 (2004)